Ecological Indicators 93 (2018) 1089–1100

Contents lists available at ScienceDirect

Ecological Indicators

journal homepage: www.elsevier.com/locate/ecolind

# A prognostic phenology model for alpine meadows on the Qinghai–Tibetan Plateau

Qingling Sun[a,b], Baolin Li[a,b,c,*], Yecheng Yuan[a], Yuhao Jiang[a,b], Tao Zhang[a,b], Xizhang Gao[a], Jinsong Ge[d], Fei Li[d], Zhijun Zhang[d]

[a] State Key Laboratory of Resources and Environmental Information System, Institute of Geographic Sciences and Natural Resources Research, Chinese Academy of Sciences, Beijing 100101, China
[b] University of Chinese Academy of Sciences, Beijing 100049, China
[c] Jiangsu Center for Collaborative Innovation in Geographical Information Resource Development and Application, Nanjing 210023, China
[d] Qinghai Remote Sensing Monitoring Center for Ecology and Environment, Xining 810007, China

ARTICLE INFO

*Keywords:*
Phenology model
Alpine meadow
Qinghai–Tibetan Plateau
Growing Season Index
Climatic factor

ABSTRACT

Phenology models are useful tools to study phenology shifts and their responses to climate change. Multiple factors including temperature, precipitation, photoperiod, insolation, and snow can affect the phenology of alpine grasslands on the Qinghai–Tibetan Plateau (QTP), but most models applied on the QTP have only considered the influences of temperature or temperature and precipitation. This study presents a multi-factor-driven phenology model, the Alpine Meadow Prognostic Phenology (AMPP) model, based on the Growing Season Index (GSI), to predict both leaf onset and offset dates of QTP alpine meadows at the community scale. Five factors including daily minimum air temperature, precipitation averaged over the previous month, photoperiod, global solar radiation, and snowfall were combined into an integrated index, the Alpine Meadow Growing Season Index, to quantify climatic limitations on foliar development of QTP alpine meadows. A case study was conducted using the observed leaf onset and offset dates of dominant species in QTP *Kobresia* meadows from 1989 to 2016. The root-mean-square errors (RMSEs) of modeled leaf onset and offset dates from the AMPP model were 6.9 d and 11.0 d, respectively, decreasing by 13.8%–48.9% and 7.6%–47.1% compared with the null model and seven other phenology models. The correlation coefficients between the predicted and observed leaf onset and offset dates were 0.75 and 0.34, respectively, higher than the 0.50–0.68 and −0.22–0.11 from other models. The RMSE ranges of predicted leaf onset and offset dates among three different sites were 2.9 d and 1.1 d, respectively, lower than or equal to the 3.6–12.4 d and the 1.1–6.9 d from other models. Results indicated that the AMPP model clearly improved the prediction accuracy and simulation of the interannual variability of leaf onset and offset dates and showed more robust simulations at different sites. Moreover, this model can be easily embedded into most ecosystem process models and applied to other alpine or subalpine grasslands once it has been adapted to their requirements.

## 1. Introduction

As an important indicator of climate change, phenology shifts of alpine vegetation on the Qinghai–Tibetan Plateau (QTP) have been a research focus during the past decade (Shen et al., 2015b). Previous work based on remote sensing investigations and field observations provided phenological data at different scales (Yu et al., 2010; Zhang et al., 2013; Zhou et al., 2014; Zhu et al., 2017). These data are essential to examine the primary cues of phenology shifts and the impacts of climate change on plant phenology using phenology models. Various phenology models have been developed since the 1970s (Schwartz, 2013). Most models, however, were developed for woody plants in temperate and boreal ecosystems (Richardson et al., 2013). Modeling work for alpine grasslands on the QTP has received considerably less attention (Chen, 2017).

Alpine meadows, dominated by perennial and deciduous short grasses, are distinct plant communities constituting the largest pastureland on the QTP. They are widely distributed in the central and eastern part of the QTP at altitudes ranging from 3200 m to 4700 m (Zhou, 2001). The habitats of QTP alpine meadows are characterized by very low temperatures, high solar radiation, and moderate water availability (Sun et al., 2017). The underlying mechanisms of

* Corresponding author at: Institute of Geographic Sciences and Natural Resources Research, Chinese Academy of Sciences, 11A Datun Road, Beijing 100101, China.
*E-mail address:* libl@lreis.ac.cn (B. Li).

https://doi.org/10.1016/j.ecolind.2018.05.061
Received 13 December 2017; Received in revised form 23 May 2018; Accepted 24 May 2018
Available online 20 June 2018
1470-160X/ 

phenology shifts of QTP alpine meadows are poorly understood at present, especially for autumn phenology (Che et al., 2014; Shen et al., 2015b). Because of the special geographical, climatic and ecological conditions of QTP alpine meadows, the factors influencing their phenology are diverse and effects of climate are complex (Chen et al., 2011; Li et al., 2016; Wang et al., 2015). For these reasons, it has been difficult to model the phenology of QTP alpine meadows accurately.

Published studies on phenology modeling involving QTP alpine meadows have been mainly constrained to the prediction of spring green-up or leaf onset dates and there has been little modeling work on autumn phenology. Among those spring phenology models proposed, most only consider the effect of temperature (Liu et al., 2017b; Shen, 2011; Zhang and Li, 1992). A few models incorporate the effects of both temperature and precipitation (Chen et al., 2015; Shen et al., 2011). Chen et al. (2015) compared the performance of the traditional thermal time model (Cannell and Smith, 1983) with two revised thermal time models which considered the effects of air temperature and precipitation to predict the green-up onset dates of herbaceous species on the QTP: they found the two revised models had better prediction accuracy for plants in alpine meadows.

Apart from temperature and precipitation which have been widely investigated, other factors also influence the phenology of alpine meadows, such as light and snow. Many studies have shown that photoperiod is important in regulating leaf flush and leaf senescence (Delpierre et al., 2009; Jeong and Medvigy, 2014; Liu et al., 2017b; White et al., 1997). Ernakovich et al. (2014) found that photoperiod can constrain spring phenology in alpine regions including the QTP. Another indicator of light is solar radiation, which is responsive to clouds and aerosols influencing surface albedo and energy partitioning (Bonan, 2002; Richardson et al., 2013). Liu et al. (2016a) showed that insolation had influences on the autumn phenology of QTP alpine grasslands. The important role played by snow in affecting the spring phenology of alpine vegetation has been universally recognized (Ide and Oguma, 2013; Julitta et al., 2014; Wang et al., 2017). However, very few models have been developed which consider the effects of light and snow in predicting the phenology of QTP alpine meadows.

A phenology model that considers multiple environmental factors and predicts both spring and autumn phenology is needed for QTP alpine meadows (Liu et al., 2017b; Shen et al., 2015b). Considering the high spatiotemporal variability of plant phenology on the QTP, the model needs to be flexible to allow primary drivers to shift or co-limit in both space and time. The Growing Season Index (GSI), a generalized, bioclimatic index proposed by Jolly et al. (2005) indicating the relative constraints of multiple environmental factors on phenology, meets these requirements. Wang et al. (2013a) used a revised GSI to estimate the start and end dates of vegetation growing seasons for an alpine meadow in an integrated ecosystem model. The revised GSI applied global solar radiation instead of photoperiod to provide the year-to-year variability of light in modeling, but it removed the effect of photoperiod in regulating plant annual phenological activity which could reduce the modeling accuracy.

In this paper, a multi-factor-driven phenology model for QTP alpine meadows, the Alpine Meadow Prognostic Phenology (AMPP) model, was established under the framework of the GSI model to provide more accurate predictions of both leaf onset and offset dates. In contrast to site species-specific phenology models, this model was established at the community scale and is primarily aimed at regional applications.

## 2. Materials and methods

### 2.1. Study sites

Three agro-meteorological stations, Henan, Qumarleb, and Gade, were used in this study. They are located in the core distribution area of QTP alpine meadows covering the gradients of increasing altitude and decreasing precipitation from east to west (Fig. 1). Among the three sites, Henan has the highest annual mean air temperature and total precipitation reflecting the relatively good hydro-thermal conditions in the eastern region of the QTP alpine meadows (Table 1). Qumarleb has the lowest annual total precipitation and highest total sunshine duration representing the western region of QTP alpine meadows which is characterized by low humidity and high insolation. Gade represents the central-southern part of the QTP alpine meadows.

All vegetation at the three study sites is *Kobresia* meadow, which is the main type of alpine meadow on the QTP. Specifically, both Qumarleb and Henan are *Kobresia pygmaea* meadows while Gade is a *Kobresia humilis* meadow. At Qumarleb, the primary species include *Kobresia pygmaea*, *Festuca ovina*, *Carex moorcroftii*, and *Poa crymophila*. The former two species are in higher proportions than the other species within the community in terms of quantity and coverage. At Henan, the dominant species is *Kobresia pygmaea* and subdominant species include *Elymus nutans*, *Puccinellia tenuiflora*, and *Scirpus distigmaticus*. The primary species at Gade include *Kobresia humilis*, *Elymus nutans*, *Festuca ovina*, and *Koeleria cristata*.

### 2.2. Phenological and meteorological data

Considering that remote sensing based phenology has significant uncertainties caused by data sources, quality, processing and extraction methods (Liu et al., 2016a; Wang et al., 2013b; Zhang et al., 2013), we used more reliable field observations at the species-level to obtain the community-level phenology through scaling in this study. Observed phenological data from 1989 to 2016 were obtained at Henan and Qumarleb, while at Gade only data from 2000 to 2012 were available. Phenological observations were conducted every two days at fixed field sites following the criteria of the China Meteorological Administration (CMA; 1993). Leaf onset was identified when 50% of ten chosen individual grasses displayed green leaves and had a height of approximately 1 cm. Leaf offset was identified when leaf coloration in 50% of the same ten grasses exceeded two thirds. The community-level phenology was acquired using the scaling method of Liang et al. (2011) and Schwartz (2013) by calculating the weighted average of the species-level phenology of primary plant species within the community. At each study site, in-situ observations of all the primary species were used (the names of the primary species are shown in Section 2.1). The weight of each species was estimated from its coverage proportion which was acquired from field investigations.

Meteorological data including daily minimum air temperature, maximum air temperature, mean air temperature, relative humidity, and total precipitation were obtained from the CMA (for Henan and Qumarleb) and the Qinghai Meteorological Bureau of China (for Gade). Soil gravimetric water content (GWC) data at the three study sites were obtained from the Qinghai Meteorological Bureau of China. VPD was calculated using the observed mean air temperature and relative humidity based on Tetens' formula (Tetens, 1930). Photoperiod was calculated using the site latitude and day of year. Since there was no observation of solar radiation at the three study sites, daylight mean global solar radiation was first estimated using a model, MT-CLIM 4.3 (freely downloaded at http://www.ntsg.umt.edu/project/mtclim), which required site-related information (i.e. latitude, elevation, slope and aspect) as well as daily maximum air temperature, minimum air temperature, and precipitation as model input data (Running et al., 1987). Then, estimated global solar radiation was further corrected using formulas acquired at the two nearest national radiation observation stations: Maqin and Yushu. Least squares linear regression between the observed and estimated global solar radiation was conducted separately at Maqin and Yushu at monthly intervals (see Supplementary Table S1). Coefficients obtained at Maqin were used to correct estimated global solar radiation at Henan and Gade, and those obtained at Yushu were used to calibrate estimated global solar radiation at Qumarleb.

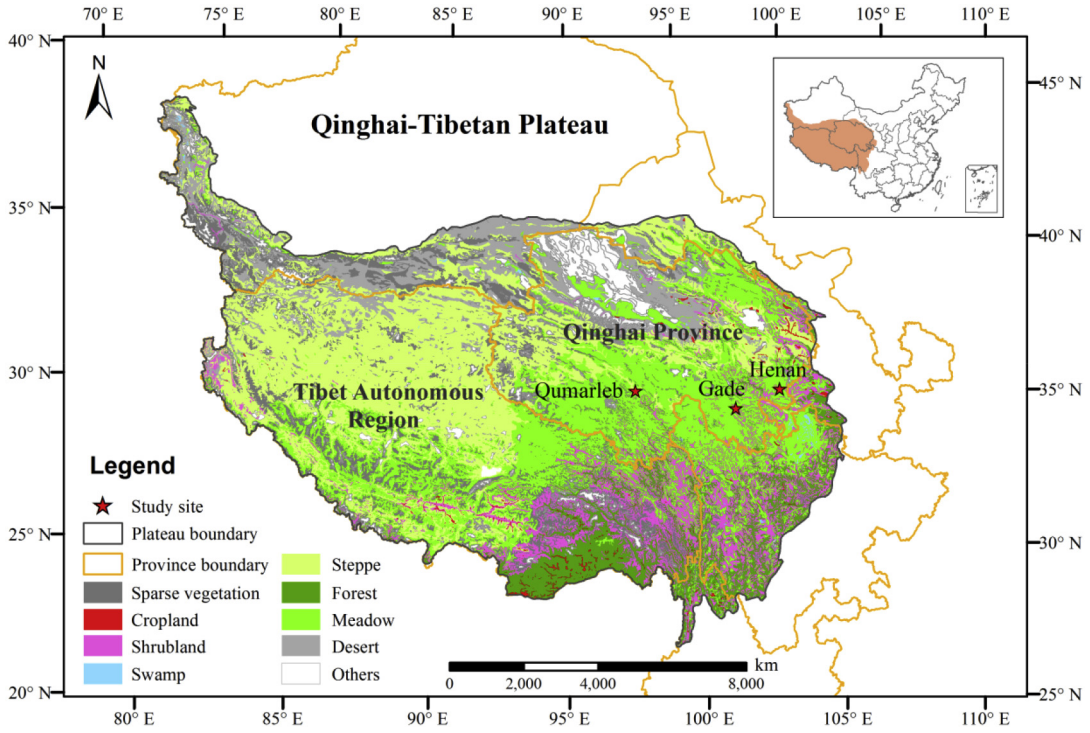


**Fig. 1.** Map showing the geographic locations of the three study sites (Henan, Qumarleb and Gade) and vegetation distribution on the QTP.

**Table 1**
Geographical coordinates, altitude, and average climatic conditions of the three study sites calculated from meteorological observations during 2000–2012. T is mean annual air temperature; P is annual total precipitation; and SD is annual total sunshine duration.

| Site | Latitude (°) | Longitude (°) | Altitude (m) | T (°C) | P (mm) | SD (h) |
|---|---|---|---|---|---|---|
| Henan | 34.73 | 101.60 | 3500 | 0.4 | 581.4 | 2636.5 |
| Qumarleb | 34.12 | 95.80 | 4175 | –1.0 | 455.6 | 2651.0 |
| Gade | 33.97 | 99.90 | 4050 | –1.7 | 536.1 | 2428.4 |

### 2.3. General idea

The general idea of this study is to develop a multi-factor-driven phenology model under the modeling framework of GSI for QTP alpine meadows. The original GSI included minimum air temperature, vapor pressure deficit (VPD) and photoperiod to reflect the constraints of temperature, humidity, and light, respectively. However, the three variables adopted by the original GSI model are not enough to interpret complex phenological changes of alpine meadows on the QTP.

The habitat of alpine meadows is characterized by high solar radiation, indicating that the growth of alpine meadow vegetation needs relatively high insolation as energy input of photosynthesis because of its low light use efficiency and chlorophyll level (Zhou, 2001). Precipitation is a critical factor affecting spring phenology of QTP alpine meadows because it is the primary source of soil water and determines water availability for plant growth (Jin et al., 2013; Li et al., 2016; Shen et al., 2015a). Moreover, Chen et al. (2015) indicated that the interactions between snowfall and temperature triggered green-up of alpine grasslands on the QTP and proposed that the influence of snow should be integrated in phenology modeling.

As discussed above, solar radiation, precipitation, and snow are all demonstrated to exert important influences on phenology of QTP alpine meadows, but they were not considered in the original GSI. Therefore, we remain the effects of temperature and photoperiod, and added influences of precipitation, insolation, and snow to establish the AMPP model. Specifically, the model is driven by five factors: daily minimum temperature ($T_{min}$), precipitation averaged over the previous month (PA), daily photoperiod (Photo), daylight mean global solar radiation (Rad), and daily snowfall (Snow).

### 2.4. Phenology modeling

Like the original GSI model (Jolly et al., 2005), individual indexes indicating the relative constraints of $T_{min}$, PA, Photo, Rad, and Snow on foliar canopy development were first calculated. They were termed as $iT_{min}$, iPA, iPhoto, iRad, and iSnow, respectively. These index values all varied between 0 (totally constrained) and 1 (totally unconstrained).

Second, multiplication of these indexes was used to form a new indicator (Eq. (1)), hereafter referred to as the AMGSI (Alpine Meadow Growing Season Index), to reflect the integrated climatic limitations on foliar development. The 11-day moving average of daily AMGSI was then applied to buffer single extreme events from prematurely triggering canopy changes. We tested a number of intervals and found no appreciable difference among the intervals varying from 11 to 21 days. A small period of 11 days was used to avoid missing the key transition points of phenophases.

Last, leaf onset date was defined as the time when the AMGSI exceeded a threshold in the spring and leaf offset date was defined as the time when the AMGSI dropped below the threshold in the autumn.

$$iAMGSI = iT_{min} \times iPA \times iPhoto \times iRad \times iSnow \quad (1)$$

- $iT_{min}$

Calculation of $iT_{min}$ was kept the same as that in Jolly et al. (2005) (Eq. (2)),

$$iTmin = \begin{cases} 0, & if\ T_{min} \leqslant T_{mmin} \\ \frac{T_{min} - T_{mmin}}{T_{mmax} - T_{mmin}}, & if\ T_{mmax} > T_{min} > T_{mmin} \\ 1, & if\ T_{min} \geqslant T_{mmax} \end{cases} \quad (2)$$

where $T_{min}$ was the observed daily minimum temperature (°C), $T_{mmin}$ and $T_{mmax}$ were the lower and upper minimum temperature thresholds,

respectively.

- iPA

Precipitation averaged over the previous month instead of VPD was used to reflect the effect of water limitation on phenology in this study. We used precipitation accumulation to represent the main source of soil water and average precipitation over the previous month as a surrogate for mean soil moisture, because soil moisture is a continuous variable and more stable than precipitation. The period of one month was determined based on the study of Shen et al. (2011) which showed that at most meteorological stations on the QTP, green-up onset dates of alpine grasslands were significantly correlated with precipitation during the previous month (Eqs. (3) and (4)),

$$PA(d) = \frac{\sum_{d-29}^{d} P(d)}{30} \tag{3}$$

$$iPA = \begin{cases} 0, & if\ PA \leqslant PA_{min} \\ \frac{PA - PA_{min}}{PA_{max} - PA_{min}}, & if\ PA_{max} > PA > PA_{min} \\ 1, & if\ PA \geqslant PA_{max} \end{cases} \tag{4}$$

where $PA$ was precipitation averaged over the previous month (mm). $d$ was the day of year and if $d$ was lower than 30, meteorological data from the last year was applied to calculate $PA$. $PA_{min}$ and $PA_{max}$ were the lower and upper thresholds of $PA$, respectively.

- iPhoto

iPhoto was directly calculated following the equation in Jolly et al. (2005) (Eq. (5)),

$$iPhoto = \begin{cases} 0, & if\ Photo \leqslant Photo_{min} \\ \frac{Photo - Photo_{min}}{Photo_{max} - Photo_{min}}, & if\ Photo_{max} > Photo > Photo_{min} \\ 1, & if\ Photo \geqslant Photo_{max} \end{cases} \tag{5}$$

where $Photo$ was daily photoperiod (h), and $Photo_{min}$ and $Photo_{max}$ were the lower and upper photoperiod thresholds, respectively.iRad

According to the studies of Stöckli et al. (2008) and Wang et al. (2013a), we also assumed in the study that daylight mean global solar radiation lower than a minimum threshold could completely limit the canopy development of alpine meadows and above another threshold could allow unconstrained canopy development (Eq. (6)),

$$iRad = \begin{cases} 0, & if\ Rad \leqslant Rad_{min} \\ \frac{Rad - Rad_{min}}{Rad_{max} - Rad_{min}}, & if\ Rad_{max} > Rad > Rad_{min} \\ 1, & if\ Rad \geqslant Rad_{max} \end{cases} \tag{6}$$

where $Rad$ was daylight mean global solar radiation (W/m$^2$), and $Rad_{min}$ and $Rad_{max}$ were the lower and upper solar radiation thresholds, respectively.

- iSnow

A two-valued function was used in this study to depict the constraint of snowfall on phenology of QTP alpine meadows following Migliavacca et al. (2011). The function had a value of 0 when there was snowfall and 1 during the snowfall-free period (Eq. (7)). Because we did not have daily snowfall data separately recorded within precipitation totals at the study sites, we assumed according to Chen et al. (2015) that snowfall occurred on days when the daily mean air temperature fell below 0 °C and there was precipitation at the same day.

$$iSnow = \begin{cases} 0, & if\ snowfall \neq 0 \\ 1, & if\ snowfall = 0 \end{cases} \tag{7}$$

### 2.5. Model fitting

Although the parameters of the AMPP model have bio-physiological dimensions that can theoretically be measured, this is rarely possible in practice because the true values of those parameters are hardly ever measured and are little known. Hence, we estimated the approximate values through mathematical optimization in this study. The whole phenological and meteorological dataset was divided into two parts: data in odd years and data in even years. One part was used to fit the model (fitting dataset) and the other part was used to validate the model (validation dataset). The model fitting was conducted twice using different fitting datasets (even-years and odd-years) which generated two sets of optimized model parameters. The best set of model parameters was selected based on the lowest total root-mean-square errors (RMSEs) between the predicted and observed leaf onset and offset dates (Eq. (8)),

$$E = \sqrt{\frac{\sum_{i=1}^{n} (OBS_i^{onset} - MOD_i^{onset})^2}{n}} + \sqrt{\frac{\sum_{i=1}^{n} (OBS_i^{offset} - MOD_i^{offset})^2}{n}} \tag{8}$$

where $E$ indicated the total RMSE and $n$ was the number of years. $OBS_i^{onset}$ and $OBS_i^{offset}$ were observed leaf onset and offset dates in the $i$th year, respectively. $MOD_i^{onset}$ and $MOD_i^{offset}$ were predicted leaf onset and offset dates in the $i$th year, respectively.

Model fitting was done using the very fast simulated annealing (VFSA) algorithm (Ingber, 1989). Parameters involved in the optimization included $T_{mmin}$, $T_{mmax}$, $PA_{min}$, $PA_{max}$, $Photo_{min}$, $Photo_{max}$, $Rad_{min}$, $Rad_{max}$, and the AMGSI threshold ($AMGSI_{thr}$). The ranges and initial values of these parameters were determined based on previous studies (Jolly et al., 2005; Larcher and Bauer, 1981; Stöckli et al., 2008) and actual variation characteristics of parameters obtained from observation data (Table 2). A constraint condition was added in the optimization that optimized parameter values indicating lower thresholds should be lower than those indicating upper thresholds. The energy function applied in the VFSA algorithm was the sum of RMSEs between predicted and observed leaf onset and offset dates (see Eq. (8)). The final optimized values of the parameters in the AMPP model are

**Table 2**
Parameters involved in the fitting of the Alpine Meadow Prognostic Phenology (AMPP) model and their optimized values. The ranges and initial values were required in the very fast simulated annealing (VFSA) algorithm to obtain optimum values.

| Parameters | Units | Meanings | Ranges | Initial values | Optimized values |
|---|---|---|---|---|---|
| $T_{mmin}$ | °C | the lower $T_{min}$ threshold | [−8.0, −1.0] | −2.0 | −7.6 |
| $T_{mmax}$ | °C | the upper $T_{min}$ threshold | [0.0,5.0] | 3.0 | 2.0 |
| $Photo_{min}$ | h | the lower Photo threshold | [10.0,12.0] | 10.5 | 11.8 |
| $Photo_{max}$ | h | the upper Photo threshold | [12.0,14.0] | 13.0 | 13.8 |
| $Rad_{min}$ | W/m$^2$ | the lower Rad threshold | [100.0,300.0] | 200.0 | 170.0 |
| $Rad_{max}$ | W/m$^2$ | the upper Rad threshold | [300.0,500.0] | 400.0 | 320.0 |
| $PA_{min}$ | mm | the lower PA threshold | [0.0,1.0] | 0.5 | 0.2 |
| $PA_{max}$ | mm | the upper PA threshold | [1.0,3.0] | 2.0 | 2.0 |
| $AMGSI_{thr}$ | / | the AMGSI threshold | [0.1,0.9] | 0.5 | 0.125 |

displayed in Table 2.

### 2.6. Model validation

To assess the AMPP model more comprehensively, we compared the performance of this model with the null model (overall mean; hereafter termed as NM) and seven other phenology models. These were the traditional thermal time model (Cannell and Smith, 1983; hereafter termed as TT), two revised TT models considering the parallel and sequential influences of air temperature and precipitation proposed by Chen et al. (2015) for QTP herbaceous plants (termed as PTT and STT, respectively), the classical model proposed by Delpierre et al. (2009) (termed as DM), the model of White et al. (1997) (referred to as WM), original GSI model proposed by Jolly et al. (2005) (referred to as GSI), and a revised GSI model which had been applied to an alpine meadow on the QTP (Wang et al., 2013a; referred to as WGSI). Among the seven models, TT, PTT and STT are spring phenology models while DM is an autumn phenology model. WM, GSI and WGSI are phenology models which can estimate not only spring leaf onset dates but also autumn leaf offset dates. Detailed definitions of these models and model parameters are shown in Supplementary Table S2.

All the models used in the comparison except for the NM were fitted following the same parameter optimization procedure described in Section 2.5 (the cost function in the VFSA algorithm may change depending on the phenophase to be predicted). The optimized parameter sets for those phenology models are listed in Supplementary Table S3. The quality of model predictions was assessed through RMSE and Pearson's correlation coefficient ($r$). The RMSE was used to describe the difference between modeled and observed phenophase dates (Eq. (9)), which was an overall accuracy measure. The $r$ was used to indicate the consistency of interannual variability or variation patterns between modeled and observed phenophase dates (Eq. (10)). The $r$ was bounded with its value ranging from −1.0 to 1.0. A model was deemed to perform better when its RMSE was relatively lower and $r$ was closer to 1.0,

$$RMSE = \sqrt{\frac{1}{n}\sum_{i=1}^{n}(OBS_i - MOD_i)^2} \quad (9)$$

$$r = \frac{\sum_{i=1}^{n}(OBS_i - \overline{OBS})(MOD_i - \overline{MOD})}{\sqrt{\sum_{i=1}^{n}(OBS_i - \overline{OBS})^2 \sum_{i=1}^{n}(MOD_i - \overline{MOD})^2}} \quad (10)$$

where $\overline{OBS}$ was the mean observed leaf onset or offset date for $n$ years and $\overline{MOD}$ was the mean modeled leaf onset or offset date for $n$ years. $OBS_i$ and $MOD_i$ were the observed and modeled phenophase dates in the $i$th year, respectively.

## 3. Results

### 3.1. Model overall accuracy

The AMPP model we proposed showed better accuracy than the NM and other phenology models including TT, PTT, STT, DM, WM, GSI, and WGSI in modeling both leaf onset and offset dates (Table 3). Specifically, the RMSE of modeled leaf onset dates based on the AMPP model was 6.9 d. The lowest and highest RMSEs based on other models were 8.0 d from the NM and 13.5 d from the WGSI. Therefore, the AMPP model decreased the RMSE of predicted leaf onset dates by 13.8%–48.9% compared with other models. The RMSE of modeled leaf offset dates based on the AMPP model was 11.0 d. The lowest RMSE based on other models was 11.9 d from the NM, and the highest RMSE was 20.8 d from the WM. Hence, the AMPP model decreased the RMSE of modeled leaf offset dates by 7.6%–47.1%. The total RMSE of the AMPP model was 17.9 d. The lowest total RMSE calculated from other models was 19.9 d from the NM, and the highest total RMSE was 31.6 d from the WM. The AMPP model decreased total RMSE by 10.1%–43.4% compared with other models.

**Table 3**
Comparison of the root-mean-square errors (RMSEs) from the Alpine Meadow Prognostic Phenology (AMPP) model and other models. The total RMSE is the sum of the RMSEs of predicted leaf onset and offset dates.

| Models | RMSE–Leaf onset (d) | RMSE–Leaf offset (d) | Total RMSE (d) |
|---|---|---|---|
| AMPP | 6.9 | 11.0 | 17.9 |
| NM | 8.0 | 11.9 | 19.9 |
| TT | 10.8 | / | / |
| PTT | 10.6 | / | / |
| STT | 10.0 | / | / |
| DM | / | 13.6 | / |
| WM | 10.8 | 20.8 | 31.6 |
| GSI | 10.9 | 12.6 | 23.5 |
| WGSI | 13.5 | 15.1 | 28.5 |

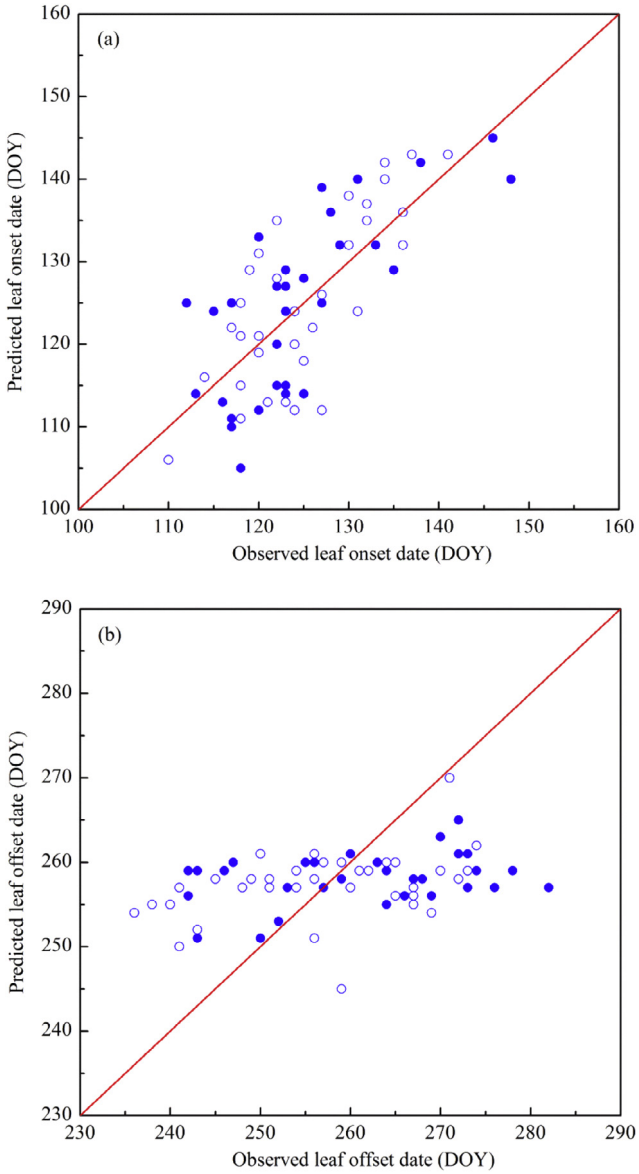


**Fig. 2.** Comparison of predicted versus observed dates of (a) leaf onset and (b) leaf offset for QTP alpine meadow communities. The hollow circles indicate the fitting dataset and the solid circles indicate the validation dataset. The red lines are the 1:1 identity lines.

Overall, the AMPP model displayed higher accuracy in predicting leaf onset dates than in predicting leaf offset dates. Fig. 2 indicates that there was no obvious systematic error associated with leaf onset or offset date estimation because points were distributed on both sides of the 1:1 line. The predicted mean leaf onset date (day of the year (DOY) 125) and its range (DOY 105 to DOY 145) were very close to the observed mean leaf onset date (DOY 125) and range (DOY 110 to DOY 148). The predicted mean leaf offset date (DOY 258) was also close to the observed mean leaf offset date (DOY 259), but the predicted range of leaf offset dates (DOY 245 to DOY 270) was clearly narrower than the observed range (DOY 235 to DOY 282). The ability of the AMPP model to predict accurately leaf offset dates was impaired by the large variability of leaf offset dates at different sites.

The GSI, WGSI and AMPP were all models of the GSI family. In comparison with the GSI and WGSI, the AMPP model decreased the total RMSE by 23.8% and 37.2%, respectively. The RMSE of predicted leaf onset dates dropped by 36.7% and 48.9%, respectively, and the RMSE of predicted leaf offset dates dropped by 12.7% and 27.2%, respectively. The improvements of the AMPP model over the GSI and WGSI were more significant in predicting leaf onset dates than in predicting leaf offset dates.

### 3.2. Interannual variability

The AMPP model outperformed other models in predicting the interannual variability of leaf onset and offset dates. Among those models, predicted leaf onset and offset dates from the NM showed no interannual variability (Fig. 3), so the NM is not discussed further regarding interannual variability. The better performance of the AMPP model in predicting interannual variability of leaf onset and offset dates can be quantitatively drawn from the correlation coefficients between modeled and observed dates (Table 4). The average $r$ of the AMPP model was 0.55 which was higher than 0.24, 0.20, and 0.28 from the WM, GSI, and WGSI, respectively. The $r$ between predicted leaf onset dates from the AMPP model and observed leaf onset dates was 0.75 which was higher than 0.50–0.68 from the TT, PTT, STT, WM, GSI, and WGSI. The $r$ between predicted leaf offset dates from the AMPP model and observed leaf offset dates was 0.34 which was also higher than −0.22 to 0.11 from the DM, WM, GSI, and WGSI. It can be seen that the interannual variability of leaf onset date was more accurately simulated compared with that of leaf offset date.

### 3.3. Intersite variability

Compared with other models, the AMPP model also displayed higher robustness in the prediction accuracy of leaf onset and offset dates among the three study sites (Table 5). The RMSE range of predicted leaf onset dates from the AMPP model was 2.9 d among the three sites, lower than the 5.9 d, 6.0 d, 4.8 d, 7.4 d, 3.6 d, 9.1 d, and 12.4 d from the NM, TT, PTT, STT, WM, GSI, and WGSI. The RMSE range of predicted leaf offset dates from the AMPP model was 1.1 d, clearly lower than 5.1 d, 6.9 d, 5.8 d, and 4.6 d from the NM, DM, WM, and GSI, and equal to 1.1 d from the WGSI. Therefore, variations in modeling accuracy of the AMPP model among three study sites were relatively small.

The AMPP model also displayed higher robustness in modeling the interannual variability of leaf onset and offset dates among different study sites than other models (Table 6). The range of $r$ values between predicted leaf onset dates from the AMPP model and observed leaf onset dates was 0.30 among the three sites. It was lower than the values of 0.40, 0.51, and 0.45 from the PTT, WM, and GSI, and similar to the 0.29, 0.31, and 0.33 from the TT, STT and WGSI. The range of $r$ values between predicted leaf offset dates from the AMPP model and observed leaf offset dates was 0.17, lower than the 0.31, 0.76, and 0.27 from the DM, WM, and GSI, and very similar to the 0.16 from the WGSI. By and large, the AMPP model has an advantage in robust simulation of the interannual variability of leaf onset and offset dates at different sites.

## 4. Discussion

### 4.1. Impacts of multiple factors in the AMPP model

#### 4.1.1. Impacts on prediction accuracy

To assess the effectiveness of each factor in the AMPP model for accurate prediction of leaf onset and offset dates, we removed one limiting factor each time from the AMPP model to obtain new GSI formulations (calculations of the remaining indexes were kept unchanged). Overall, the five factors used in the AMPP model were all useful in accurately predicting leaf onset and offset dates because RMSEs of predicted leaf onset and offset dates from those new GSI formulations were all not lower than those from the AMPP model (Table 7).

Overall, PA and $T_{min}$ showed the strongest influences on the prediction accuracy of leaf onset date. When the influences of PA and $T_{min}$ were excluded, the RMSEs of predicted leaf onset dates increased by 9.7 d and 8.7 d, respectively (Table 7). The effects of Photo and Snow on the unbiased estimation of leaf onset dates were also very positive, though their influences were not as significant as those of PA and $T_{min}$. Rad displayed no obvious influence on the estimation of leaf onset dates. Photo was the most important factor in accurately estimating leaf offset dates and excluding its influence increased the RMSE of predicted leaf offset dates by 25.8 d. $T_{min}$ and Rad also played important roles in predicting leaf offset dates and including them in the AMPP model decreased the RMSEs of modeled leaf offset dates by 1.3 d and 1.0 d, respectively. PA in the model also had a positive influence on the prediction of leaf offset dates. Snow mainly affected the accurate estimation of leaf onset dates and its influence on the prediction of leaf offset dates was negligible.

Fundamentally, different limitations of the factors used in the AMPP model within a year caused the primary factors limiting spring leaf onset and autumn leaf offset to be distinctly different. On average, the limitations of $T_{min}$ and PA were strongest in the spring (Fig. 4). In the autumn, Photo was most obvious limitation, leading to the rapid decrease of AMGSI curves. Jin et al. (2013) found a latitudinal effect on the autumn phenology of alpine vegetation on the QTP which reflected mainly the influence of photoperiod. Hence, Photo was of great importance in regulating annual leaf offset, especially at large scales. Compared with the other factors in the AMPP model, snowfall limitations were not so prominent, but the influence of snowfall in the early spring on leaf onset was significant (Fig. 4).

The diverse limitations of multiple factors in the AMPP model at different sites reflected the intersite differences of climatic conditions, which also explained the robustness of the modeling accuracy in space. Among three study sites, the limitation of PA was strongest at Qumarleb (Fig. 4). As found by Shen et al. (2011) and Shen et al. (2015a), the effect of precipitation on spring phenology is more prominent in high-aridity areas. Therefore, PA had a more important influence on the prediction of leaf onset dates than other factors at the very dry Qumarleb site. The influences of temperature and snowfall during spring were most obvious at Gade because Gade had very low air temperature and relatively high precipitation (Table 1). At Henan, although the limitation of $T_{min}$ was stronger than that of PA during most times of the year, the effects of $T_{min}$ and PA on prediction of leaf onset dates were actually close since hydro-thermal conditions at Henan were generally best among the three sites.

We can infer from the above analyses that the RMSE of TT in predicting leaf onset dates was high because it only considered the effect of forcing air temperature (Table 3). PTT and STT showed higher accuracy in comparison with TT because they considered the effects of both precipitation and air temperature on spring phenology. WM also included effects of both temperature and precipitation, but its RMSE in predicting leaf onset dates was higher than those of STT and PTT. This

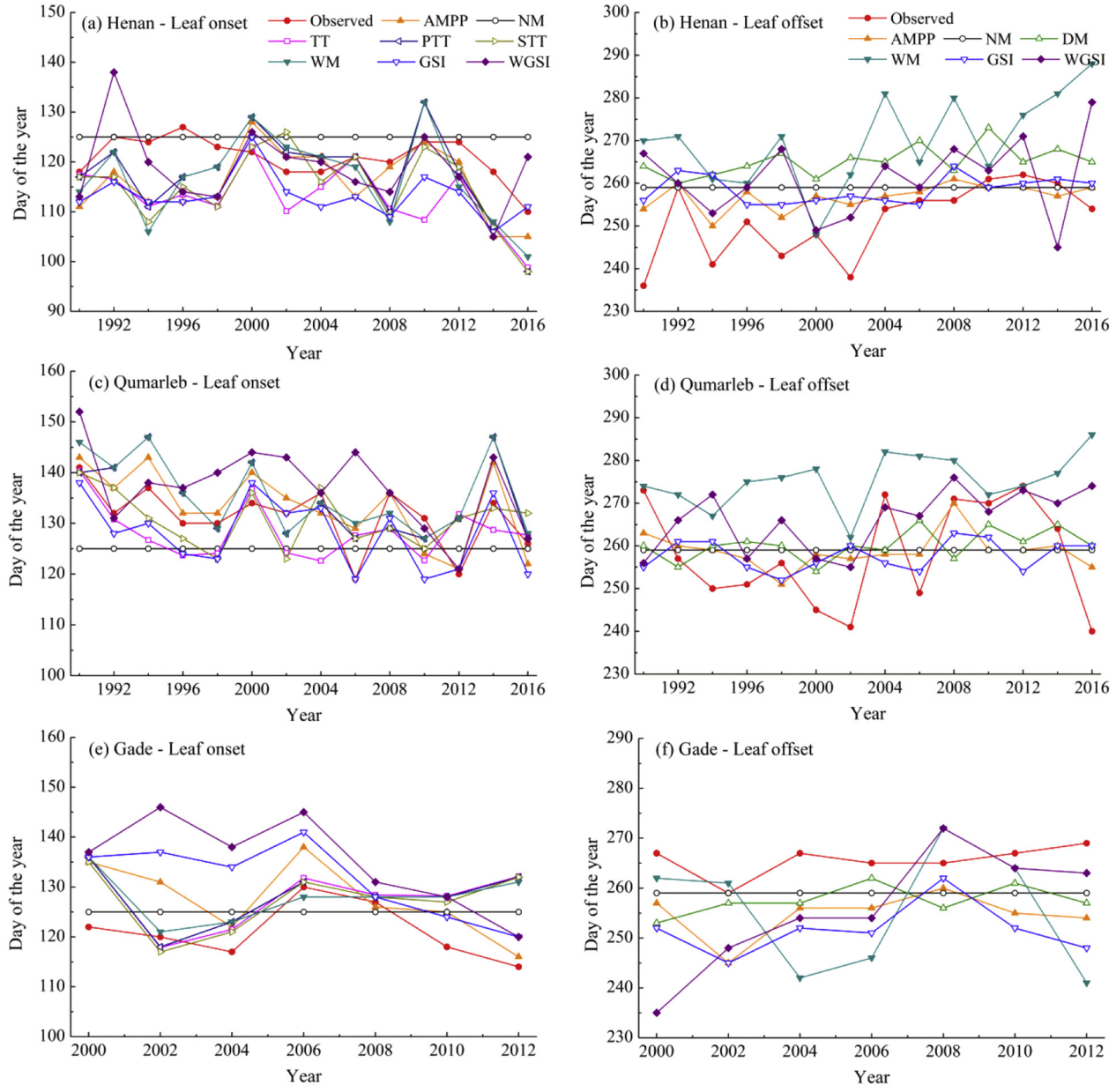


**Fig. 3.** Comparison of the interannual variability of predicted leaf onset and offset dates from different models with the variability of observations at Henan, Qumarleb, and Gade sites.

**Table 4**
Comparison of *r* values from the AMPP model and those from other models. The average *r* is the mean value of *r* for leaf onset and offset dates. The asterisk superscripts "*", "**", and "***" indicate significant correlations with confidence levels of 90%, 95%, and 99%, respectively.

| Models | *r*–Leaf onset | *r*–Leaf offset | Average *r* |
|---|---|---|---|
| AMPP | 0.75*** | 0.34** | 0.55*** |
| TT | 0.50*** | / | / |
| PTT | 0.68*** | / | / |
| STT | 0.60*** | / | / |
| DM | / | –0.22 | / |
| WM | 0.68*** | –0.07 | 0.31* |
| GSI | 0.59*** | 0.04 | 0.32* |
| WGSI | 0.58*** | 0.11 | 0.35** |

**Table 5**
Comparison of the RMSEs from the AMPP model and other models at different sites. Variations in the RMSEs from the AMPP model were relatively small among the three study sites.

| Models | RMSE–Leaf onset (d) | | | RMSE–Leaf offset (d) | | |
|---|---|---|---|---|---|---|
| | Henan | Qumarleb | Gade | Henan | Qumarleb | Gade |
| AMPP | 8.0 | 5.1 | 7.8 | 10.5 | 11.6 | 10.9 |
| NM | 4.0 | 8.2 | 9.9 | 11.4 | 12.5 | 7.4 |
| TT | 11.4 | 8.1 | 14.1 | / | / | / |
| PTT | 10.1 | 9.1 | 13.9 | / | / | / |
| STT | 10.9 | 6.2 | 13.6 | / | / | / |
| DM | / | / | / | 16.1 | 12.7 | 9.2 |
| WM | 10.4 | 9.7 | 13.3 | 21.3 | 22.2 | 16.4 |
| GSI | 10.0 | 7.6 | 16.7 | 10.5 | 13.0 | 15.1 |
| WGSI | 8.1 | 13.3 | 20.5 | 15.0 | 15.0 | 16.1 |

**Table 6**
Comparison of *r* values from the AMPP model and other models at different sites. The asterisk superscripts "*", "**", and "***" indicate significant correlations with the confidence levels of 90%, 95%, and 99%, respectively.

| Models | *r*–Leaf onset | | | *r*–Leaf offset | | |
|---|---|---|---|---|---|---|
| | Henan | Qumarleb | Gade | Henan | Qumarleb | Gade |
| AMPP | 0.47* | 0.77*** | 0.77** | 0.58** | 0.48* | 0.65 |
| TT | 0.50* | 0.21 | 0.24 | / | / | / |
| PTT | 0.58** | 0.55** | 0.18 | / | / | / |
| STT | 0.46* | 0.42 | 0.15 | / | / | / |
| DM | / | / | / | 0.27 | 0.13 | –0.04 |
| WM | 0.47* | 0.59** | 0.08 | 0.39 | 0.10 | –0.37 |
| GSI | 0.34 | 0.79*** | 0.61 | 0.40 | 0.13 | 0.27 |
| WGSI | 0.21 | 0.49* | 0.54 | 0.14 | 0.30 | 0.20 |

**Table 7**
Influences of different driving factors in the AMPP model on accurate prediction of leaf onset and offset dates. AMPP-$_{iTmin}$, AMPP-$_{iPA}$, AMPP-$_{iPhoto}$, AMPP-$_{iRad}$, and AMPP-$_{iSnow}$ are new formulations and each formulation includes four of the five climatic indexes in the AMPP model, excluding $iT_{min}$, iPA, iPhoto, iRad, and iSnow, respectively.

| Formulations | RMSE–Leaf onset (d) | RMSE–Leaf offset (d) | Total RMSE (d) |
|---|---|---|---|
| AMPP | 6.9 | 11.0 | 17.9 |
| AMPP$_{-iTmin}$ | 15.6 | 12.3 | 27.9 |
| AMPP$_{-iPA}$ | 16.6 | 11.7 | 28.3 |
| AMPP$_{-iPhoto}$ | 8.5 | 36.8 | 45.3 |
| AMPP$_{-iRad}$ | 7.0 | 12.0 | 19.0 |
| AMPP$_{-iSnow}$ | 7.6 | 11.0 | 18.6 |

**Table 8**
Influences of different driving factors in the AMPP model on modeling the interannual variability of leaf onset and offset dates. The asterisk superscripts "*", "**", and "***" indicate significant correlations with confidence levels of 90%, 95%, and 99%, respectively.

| Formulations | *r*–Leaf onset | *r*–Leaf offset | Average *r* |
|---|---|---|---|
| AMPP | 0.75*** | 0.34** | 0.55*** |
| AMPP$_{-iTmin}$ | 0.63*** | 0.14 | 0.39** |
| AMPP$_{-iPA}$ | 0.57*** | 0.22 | 0.40** |
| AMPP$_{-iPhoto}$ | 0.74*** | 0.30* | 0.52** |
| AMPP$_{-iRad}$ | 0.74*** | 0.15 | 0.45*** |
| AMPP$_{-iSnow}$ | 0.71*** | 0.34* | 0.53*** |

was mainly because WM used a normalized step function to match the requirements of both cool and warm grasslands (White et al., 1997). This function was not suitable for QTP alpine meadows growing in cold areas with no considerable temperature difference. For prediction of leaf offset dates, WM only considered the effect of low temperature which led to poor prediction accuracy. The AMPP model outperformed WGSI and GSI in the prediction accuracy of leaf offset dates mainly because it included both Photo and Rad which all had important influences on autumn phenology.

#### 4.1.2. Impacts on modeling interannual variability

Similarly, to assess the effect of each factor in the AMPP model on simulating the interannual variability of leaf onset and offset dates, we removed one limiting factor each time from the AMPP model to obtain new GSI formulations and correlation coefficients between newly predicted leaf onset and offset dates from those new GSI formulations and observed dates. Overall, the five factors included in the AMPP model all

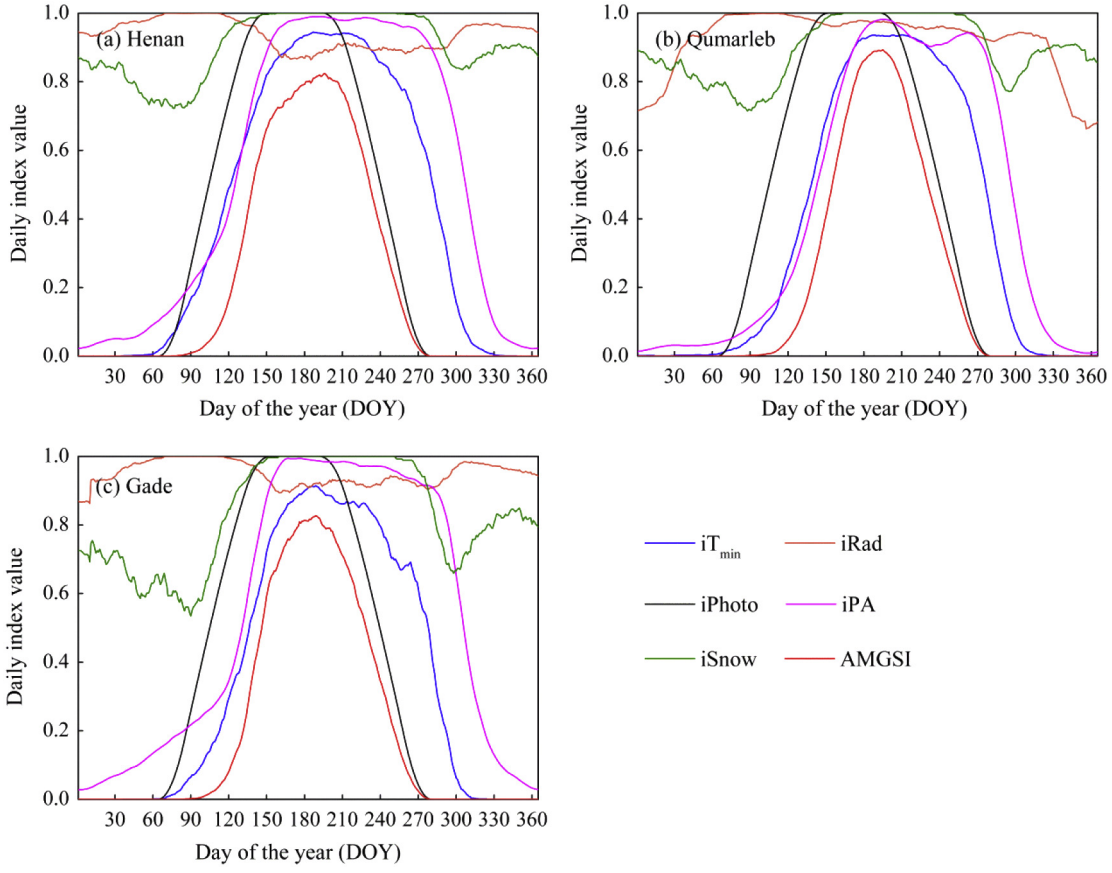


**Fig. 4.** Multi-year averaged annual variations of the five limiting indexes ($iT_{min}$, iPA, iPhoto, iRad, and iSnow) and the AMGSI at (a) Henan, (b) Qumarleb, and (c) Gade sites.

contributed positively to accurate simulation of the interannual variability of leaf onset and offset dates at different sites (Table 8). Although Photo itself had no interannual variation, it affected variations of predicted leaf onset and offset dates because all the factors interacted in the AMPP model.

Precipitation and temperature (i.e. PA and $T_{min}$) mainly controlled the interannual variability of predicted leaf onset dates. When the influences of PA and $T_{min}$ were excluded, *r* values between predicted and observed leaf onset dates decreased by 0.18 and 0.12, respectively (Table 8). The effect of PA was more significant than that of $T_{min}$ at our study sites. This is consistent with the results of Li et al. (2016) who also reported more significant correlations between leaf onset dates of dominant species in *Kobresia* meadows on the QTP and preseason precipitation at similar study sites. Light conditions indicated by Photo and Rad showed little effect on the interannual variability of leaf onset dates. Compared with PA, $T_{min}$ and Rad contributed more to accurate simulation of the interannual variations in leaf offset dates. Influences of $T_{min}$ and Rad on the interannual variability of predicted leaf offset dates were nearly equally important. Excluding $T_{min}$ and Rad from the AMPP model decreased *r* values between predicted and observed leaf offset dates by 0.20 and 0.19, respectively.

The reason that the AMPP model performed better in simulating the interannual variability of leaf onset dates than leaf offset dates can be seen in the variability of the AMGSI during spring and autumn. AMGSI during spring had obvious interannual variability at different sites which guaranteed a wide variation range of predicted leaf onset dates (Fig. 5). However, the interannual variability of AMGSI during autumn was limited by the strong effect of Photo which has no interannual variation and small intersite variability. As a result, both the interannual and intersite variability of AMGSI during autumn were much smaller (Fig. 5). The predicted leaf offset dates based on the AMGSI also had a smaller variation range and lower variability than those of leaf onset dates (Figs. 2 and 3).

Among the models involved in this study, TT had the poorest simulation of the interannual variability of leaf onset dates probably because it only considered the influence of low temperature and neglected the important effects of precipitation or water (Table 4). The *r* from PTT was higher than that from STT because the effects of air temperature and precipitation are sequential in the STT. This means that only one factor was functioning at a given point in time for STT, while the interannual variability of predicted leaf onset dates from PTT was co-determined by forcing air temperature and precipitation. For the prediction of leaf offset dates, DM included the influences of low temperature and photoperiod, but did not consider the effects of insolation and moisture which probably explain why the *r* from DM was lower than that from the AMPP model. WM only modeled the effect of low temperature on leaf offset which could only explain small variations in leaf offset dates, so the interannual variability of predicted leaf offset dates from WM was also very poor.

### 4.2. Using PA instead of VPD to indicate water limitation

The VPD is an index used in the original GSI and WGSI to indicate the water limitation on plant phenological development. It was used as a surrogate for precipitation and ultimately for soil water content (Jolly et al., 2005). However, the effectiveness of VPD as a surrogate for precipitation and soil water content was not obvious at our study sites. Our correlation analyses showed that there was no significant correlation between VPD and precipitation at the three sites. To assess the ability of VPD to indicate soil water content, soil GWC data (surface 0–10 cm) recorded on roughly a 10-day scale during the growing seasons from 2007 to 2010 were acquired at the three sites. We can see from Fig. 6 that the patterns of VPD and GWC did not show a consistent negative correlation. A significant correlation between VPD and GWC was reported at Henan ($r = -0.43$, $p < 0.01$, $n = 53$). Correlations between VPD and GWC were weakly significant at Gade ($r = -0.21$, $p < 0.1$, $n = 84$) and not significant at Qumarleb ($r = -0.15$, $p > 0.1$, $n = 54$).

As a continuous variable, PA retained the general pattern of precipitation and also reflected the variations in soil water content (Fig. 6). Significant correlations between PA and GWC were found at all the study sites. At Henan, the correlation between PA and GWC ($r = 0.71$, $p < 0.01$, $n = 53$) was significantly higher than that between precipitation and GWC ($r = 0.27$, $p < 0.05$, $n = 53$) as well as the correlation between VPD and GWC. At Qumarleb and Gade, significant correlations between PA and GWC ($r = 0.52$, $p < 0.01$, $n = 54$ for Qumarleb; $r = 0.48$, $p < 0.01$, $n = 84$ for Gade) were also higher than those between precipitation and GWC ($r = 0.25$, $p < 0.1$, $n = 54$ for Qumarleb; $r = 0.37$, $p < 0.01$, $n = 84$ for Gade) and between VPD and GWC. Therefore, PA in the model was a better index than VPD and precipitation to indicate the water limitation.

To further test the advantage of PA over VPD in predicting leaf onset and offset dates of QTP alpine meadows, we created a new GSI formulation consisting of $T_{min}$, PA, and Photo (using PA to replace VPD in the GSI). The new GSI formulation was also fitted and validated as for the GSI. The RMSEs of predicted leaf onset and offset dates from this new GSI formulation were 9.0 d and 12.2 d, respectively, which were lower than 10.9 d and 12.6 d from the GSI (Table 3). The *r* values between predicted and observed leaf onset and offset dates were 0.69 and 0.10, respectively, all higher than 0.59 and 0.04 from the GSI (Table 4). Therefore, both the accuracy and interannual variability of predicted leaf onset and offset dates were improved using PA instead of VPD, especially for predicted leaf onset dates. This was also the main reason for better performance of the AMPP model over the GSI and WGSI in predicting leaf onset dates.

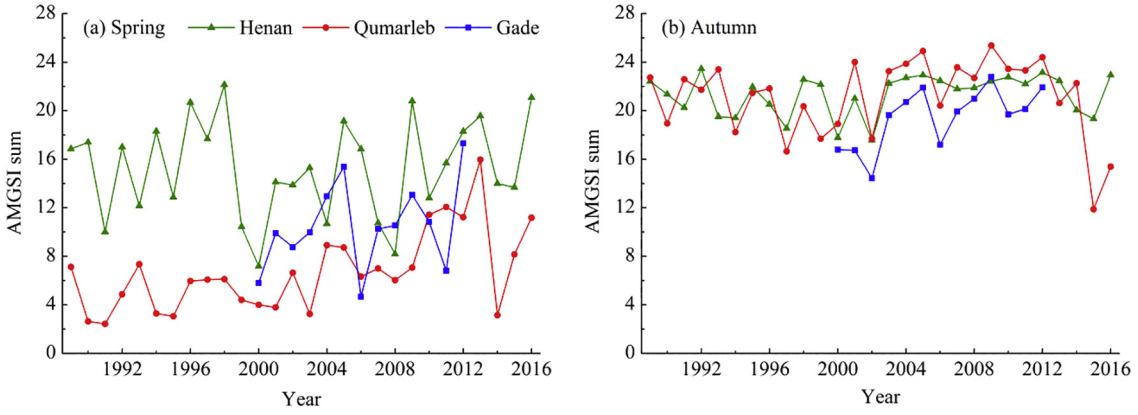


**Fig. 5.** Comparison of the interannual variability of the AMGSI sums during spring (March–May) and autumn (August–October) at Henan, Qumarleb, and Gade sites.

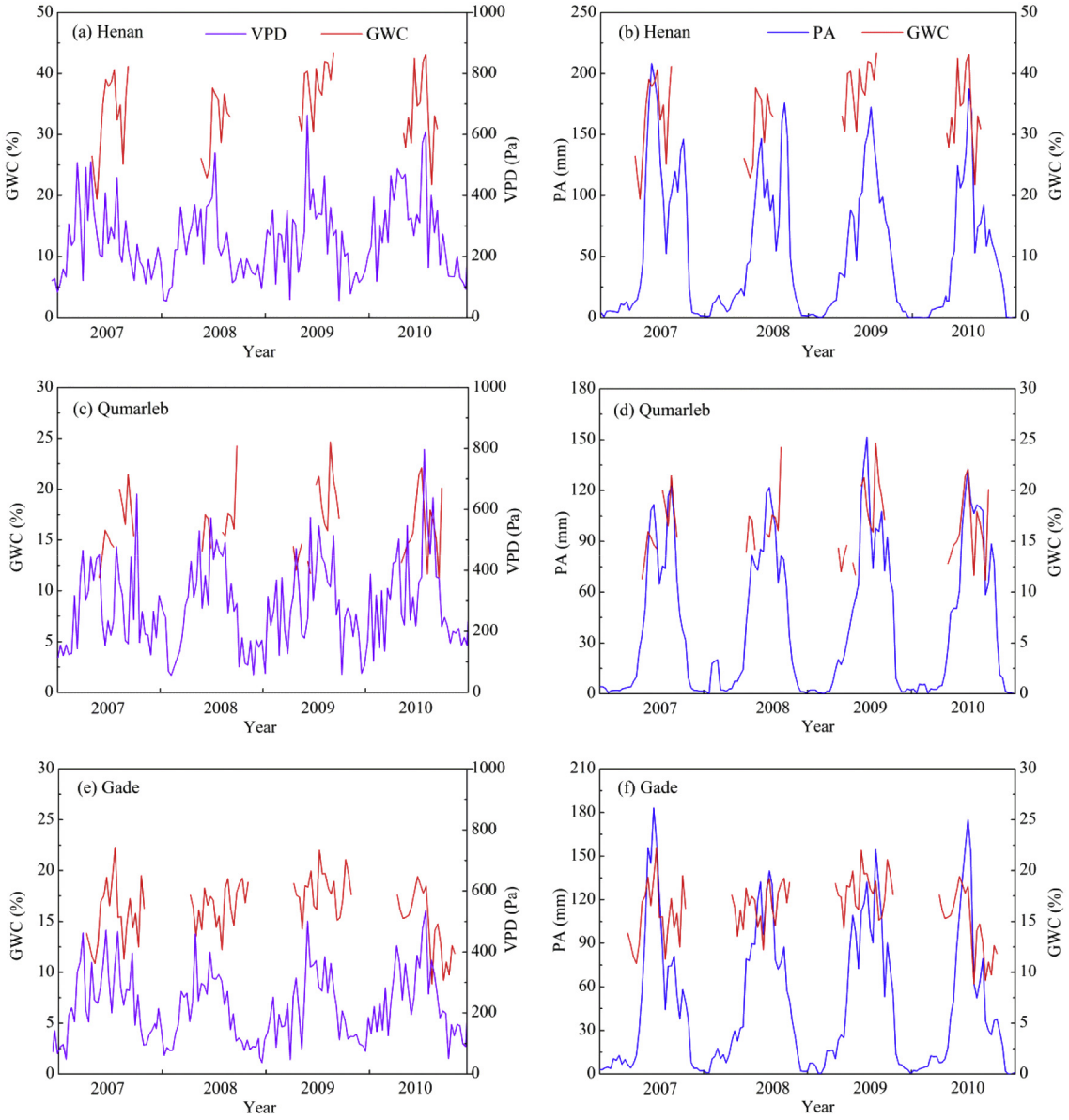


**Fig. 6.** Patterns of vapor pressure deficit (VPD), precipitation averaged over the previous month (PA), and soil gravimetric water content (GWC) during 2007–2010 at Henan, Qumarleb, and Gade. The daily VPD and PA data were sampled at roughly a 10-day interval to match the GWC record.

### *4.3. Using both Photo and Rad to indicate light constraint*

In the AMPP model, we used both Photo and Rad to reflect the impacts of light on phenology of QTP alpine meadow communities. From Section 4.1, we learned that Photo was helpful to the accurate prediction of leaf onset and offset dates, particularly for leaf offset dates. Rad had little effect on estimation of leaf onset dates, but it had an important influence on accurate prediction of leaf offset dates. For leaf offset dates, it seemed that Photo had a more important influence on the prediction accuracy while Rad had a more obvious influence on simulation of the interannual and intersite variability.

Comparison of modeling accuracy between the GSI and WGSI indicated that Photo had a greater influence on prediction accuracy of leaf offset dates than Rad (Table 3). However, including Photo in GSI family models is expected to decrease the interannual and intersite variations of predicted leaf offset dates because Photo can attenuate the interannual and intersite variability of other driving factors under the GSI framework. Removing the influence of Photo can increase the variation range of predicted leaf offset dates. We found that variation ranges of predicted leaf offset dates from the WM and WGSI were larger than those from the DM, GSI and AMPP, and thus were closer to the observed range. This was because only WM and WGSI did not include the effect of Photo among models estimating autumn phenology. Therefore, Photo included in the AMPP model led to small variability of predicted leaf offset dates, but removing the influence of Photo obviously impaired the prediction accuracy and did not improve the simulated interannual variability of leaf offset dates (Tables 7 and 8).

Compared with Photo, Rad had more important and positive influences on accurate simulation of the interannual variability of leaf offset dates. A higher $r$ from the WGSI than that from the GSI in predicting leaf offset dates supports this view (Table 4). Predicted leaf offset dates from the WM and WGSI had close variation ranges, but the $r$ from WGSI was obviously higher than that from WM. This was mainly because WGSI included the effect of Rad which affected the interannual variability of leaf offset dates at different sites. Stöckli et al. (2008) and Wang et al. (2013a) also reported that Rad could better reflect the influence of light on the interannual variability of plant phenology compared with Photo.

Photo plays a critical role in regulating annual leaf offset and it has been commonly used in phenology models including the DM and GSI. Since Photo is determined by a function of latitude and day of year, it alone cannot explain the interannual variations in leaf offset date. Its effect is likely to stabilize leaf offset date for a particular location. Rad is an integrated measure of day length and light intensity (Liu et al., 2016b), and it has obvious interannual variability. Rad is closely related to the photosynthetic active radiation (PAR), and higher Rad can enhance photosynthetic capacity and $CO_2$ sequestration rate leading to the delay of leaf offset date (Liu et al., 2016a,b). Moreover, Rad has an important influence on the stomata aperture which was reported to be the principal controlling agent in leaf senescence (Thimann and Satler, 1979a,b). Increase in insolation can retard the accumulation of abscisic acid that is paralleled by stomatal closure, and subsequently slow the speed of leaf senescence (Gepstein and Thimann, 1980; Liu et al., 2016a,b). Using both Photo and Rad in phenology modeling for QTP alpine meadows is demonstrated to be a better choice than using only one of them.

### 4.4. Uncertainties of the model

There are some uncertainties in our study that need to be highlighted. First, we acquired parameter values in the AMPP model through mathematical optimization because the theoretical values of those model parameters are seldom obtained. Optimized values are expected to be close to the true values but may be not equal to them. Additionally, the same parameter values were used to predict both leaf onset and offset dates under the GSI modeling framework. However, parameter values used to determine leaf onset and offset dates may be different (Figs. 2 and 5). The cost function used in the parameter optimization procedure only guaranteed that the total prediction error of leaf onset and offset dates was minimized, and thus derived parameter values may be not optimal for each phenophase prediction. We once conducted an experiment to explore the influences of one AMGSI threshold and two different thresholds on prediction of leaf onset and offset dates. It showed that the predicted results were not significantly different but optimized parameter values were changed slightly. So we used a single AMGSI threshold to decrease model parameters.

Second, only climatic forces were considered in the model because we wanted to establish a prognostic phenology model which could predict the influences of climate change on phenology shifts of QTP alpine meadows. However, foliar phenology of QTP alpine meadows may also be influenced by other factors, such as grassland degradation, soil thaw-freeze processes, plant community succession, nitrogen deposition, and physical damage (Chen et al., 2011; Liu et al., 2017a). This study showed that the five factors in the AMPP model cannot totally explain variations in leaf onset and offset dates, especially leaf offset dates. Moreover, responses of plant phenological activity to climatic forces (i.e. functions for calculating climatic indexes used in the model) were all assumed to be linear in this study following Jolly et al. (2005). Actually, those indexes probably follow non-linear curves (Shen et al., 2015b; Wang et al., 2015), and the AMPP model may be further improved by addressing the non-linear relations. Therefore, future work is still needed to explore the underlying driving factors and their influencing mechanisms on phenology shifts of QTP alpine meadow communities.

Finally, the model was only tested at three sites owing to data availability and applicability. Valid and accurate data at more sites across the whole distribution area of alpine meadows on the QTP is expected to boost the model. However, long-term phenological observation sites in alpine meadow distribution areas are limited on the QTP (Chen et al., 2015; Zhu et al., 2017). The ground-based phenological data we acquired were from the CMA which has the largest phenological observation network in China. There are only five CMA stations with meadow vegetation on the QTP. They are Henan, Qumarleb and Gade in the Qinghai province, and Zoige and Shiqu in the Sichuan province. However, vegetation at Zoige is swamp meadow which is not typical alpine meadow and Shiqu has no phenological record of the dominant grass species (Zheng et al., 2016). Therefore, only data at Henan, Qumarleb and Gade were used in our study.

### 4.5. Advantage and extensibility of the model

This study provided a multi-factor-driven phenology model to predict leaf onset and offset dates of QTP alpine meadows. Five factors were included in the model and all of them were demonstrated to be useful in accurately predicting leaf onset and offset dates at our study sites. Compared with other phenology models which generally include no more than three driving factors, the multi-factor-driven AMPP model displayed better performance in terms of both prediction accuracy and simulation of the interannual variability. This indicates that using those multiple factors improves phenology modeling for alpine meadows on the QTP and advantage of this model is expected to be clearer when applied at larger spatial scales.

The flexible modeling framework is also one of advantages of the AMPP model. The GSI framework makes it very flexible to add or replace environmental factors. Factors controlling leaf onset and offset can be integrated into a phenology model and different factors play different roles in different phenophases. It does not impose a priori knowledge of the vegetation or climate to switch discretely between models or model parameters. It simply allows primary limiting factors to shift or co-limit both temporally and spatially and uses a common set of parameters that do not vary by site, which is essential to the regional simulation of leaf onset and offset dates.

Although the aim of this research was to establish a prognostic phenology model adapted to alpine meadow communities on the QTP, the model we proposed can also be applied to other alpine or subalpine grasslands once adapted to their particular requirements. Moreover, the AMPP model can be embedded into most ecosystem process models applied at regional scale because of its simplicity. Therefore, the model has obvious advantages, and more importantly, good extrapolation possibilities. Regional simulations based on this model and predictions of phenology shifts under future climate scenarios will be the foci of our future work.

## 5. Conclusions

A new phenology model, the AMPP model, was proposed in this study to predict both leaf onset and offset dates of QTP alpine meadows at the community scale. A case study based on the observed leaf onset and offset dates of dominant species in *Kobresia* meadows at three sites from 1989 to 2016 was conducted. Comprehensive model validation assessing prediction accuracy as well as simulation of the interannual variability showed that the AMPP model provided more reliable predictions of both leaf onset and offset dates than the NM, TT, PTT, STT, DM, WM, GSI, and WGSI. Besides, the AMPP model also displayed more robust simulations at different sites which indicated that the model has very good extrapolation ability at the regional scale.

The AMPP model outperformed the NM, TT, PTT, STT, DM, and WM mainly because it included the influences of multiple factors affecting the interannual and intersite variability of leaf onset and offset dates. Improvements of the AMPP model over the GSI and WGSI were primarily derived from the substitution of PA for VPD to indicate the water limitation and the combination of Photo and Rad to indicate light impacts. The performance of the AMPP model was also related to the GSI framework, which allows primary limiting factors to shift or co-limit both temporally and spatially. Because of its simplicity, the AMPP model can be easily embedded into most ecosystem process models and applied to other alpine or subalpine grasslands once adapted to their particular requirements.

## Acknowledgements

This work was supported by the National Key Research and Development Plan of China (grant no. 2016YFC0500205) and the National Basic Research Program of China (grant no. 2015CB954103). Sponsors are the Ministry of Science and Technology, China. We thank Huakun Zhou at Northwest Institute of Plateau Biology, CAS for providing instructions on phenological data acquisition and processing. Thanks also to A-Xing Zhu and Ken Keefover-Ring in the University of Wisconsin-Madison, USA for their advice on writing this paper. We also thank two anonymous reviewers for their helpful comments on this paper.

## Appendix A. Supplementary data

Supplementary data associated with this article can be found, in the online version, at http://dx.doi.org/10.1016/j.ecolind.2018.05.061.

## References

Bonan, G.B., 2002. Ecological Climatology: Concepts and Applications. Cambridge University Press, Cambridge, UK.
Cannell, M.G.R., Smith, R.I., 1983. Thermal time, chill days and prediction of budburst in *Picea-sitchensis*. J. Appl. Ecol. 20, 951–963.
Che, M., Chen, B., Innes, J.L., Wang, G., Dou, X., Zhou, T., Zhou, T., Zhang, H., Yan, J., Xu, G., Zhao, H., 2014. Spatial and temporal variations in the end date of the vegetation growing season throughout the Qinghai-Tibetan Plateau from 1982 to 2011. Agric. For. Meteorol. 189–190, 81–90.
Chen, X., 2017. Spatiotemporal processes of plant phenology—simulation and prediction. Springer, Berlin.
Chen, X., An, S., Inouye, D.W., Schwartz, M.D., 2015. Temperature and snowfall trigger alpine vegetation green-up on the world's roof. Glob. Change Biol. 21, 3635–3646.
Chen, H., Zhu, Q., Wu, N., Wang, Y., Peng, C.H., 2011. Delayed spring phenology on the Tibetan Plateau may also be attributable to other factors than winter and spring warming. Proc. Natl. Acad. Sci. U.S.A. 108, E93.
China Meteorological Administration, 1993. Observation Criterion of Agricultural Meteorology. China Meteorological Press, Beijing (in Chinese).
Delpierre, N., Dufrêne, E., Soudani, K., Ulrich, E., Cecchini, S., Boé, J., Francois, C., 2009. Modelling interannual and spatial variability of leaf senescence for three deciduous tree species in France. Agric. For. Meteorol. 149, 938–948.
Ernakovich, J.G., Hopping, K.A., Berdanier, A.B., Simpson, R.T., Kachergis, E.J., Steltzer, H., Wallenstein, M.D., 2014. Predicted responses of arctic and alpine ecosystems to altered seasonality under climate change. Glob. Change Biol. 20, 3256–3269.
Gepstein, S., Thimann, K.V., 1980. Changes in the abscisic acid content of oat leaves during senescence. Proc. Natl. Acad. Sci. U.S.A. 77, 2050–2053.
Ide, R., Oguma, H., 2013. A cost-effective monitoring method using digital time-lapse cameras for detecting temporal and spatial variations of snowmelt and vegetation phenology in alpine ecosystems. Ecol. Inf. 16, 25–34.
Ingber, L., 1989. Very fast simulated re-annealing. Math. Comput. Modell. 12, 967–973.
Jeong, S.J., Medvigy, D., 2014. Macroscale prediction of autumn leaf coloration throughout the continental United States. Glob. Ecol. Biogeogr. 23, 1245–1254.
Jin, Z., Zhuang, Q., He, J.S., Luo, T., Shi, Y., 2013. Phenology shift from 1989 to 2008 on the Tibetan Plateau: an analysis with a process-based soil physical model and remote sensing data. Clim. Change 119, 435–449.
Jolly, W.M., Nemani, R., Running, S.W., 2005. A generalized, bioclimatic index to predict foliar phenology in response to climate. Glob. Change Biol. 11, 619–632.
Julitta, T., Cremonese, E., Migliavacca, M., Colombo, R., Galvagno, M., Siniscalco, C., Rossini, M., et al., 2014. Using digital camera images to analyse snowmelt and phenology of a subalpine grassland. Agric. For. Meteorol. 198–199, 116–125.
Larcher, W., Bauer, H., 1981. Ecological significance of resistance to low temperature. Encyclopedia of Plant Physiology, vol. 12A Springer-Verlag, Berlin.
Li, R., Luo, T., Mölg, T., Zhao, J., Li, X., Cui, X., Du, M., Tang, Y., 2016. Leaf unfolding of Tibetan alpine meadows captures the arrival of monsoon rainfall. Sci. Rep. 6, 20985.
Liang, L., Schwartz, M.D., Fei, S., 2011. Validating satellite phenology through intensive ground observation and landscape scaling in a mixed seasonal forest. Remote Sens. Environ. 115, 143–157.
Liu, Q., Fu, Y.H., Zeng, Z., Huang, M., Li, X., Piao, S., 2016a. Temperature, precipitation, and insolation effects on autumn vegetation phenology in temperate China. Global Change Biol. 22, 644–655.
Liu, Q., Fu, Y.H., Zhu, Z., Liu, Y., Liu, Z., Huang, M., Janssens, I.A., Piao, S., 2016b. Delayed autumn phenology in the Northern Hemisphere is related to change in both climate and spring phenology. Glob. Change Biol. 22, 3702–3711.
Liu, Q., Fu, Y.H., Liu, Y., Janssens, I.A., Piao, S., 2017b. Simulating the onset of spring vegetation growth across the Northern Hemisphere. Glob. Change Biol. 97, 19–27.
Liu, L., Monaco, T.A., Sun, F., Liu, W., Gan, Y., Sun, G., 2017a. Altered precipitation patterns and simulated nitrogen deposition effects on phenology of common plant species in a Tibetan Plateau alpine meadow. Agric. For. Meteorol. 236, 36–47.
Migliavacca, M., Galvagno, M., Cremonese, E., Rossini, M., Meroni, M., Sonnentag, O., Cogliati, S., et al., 2011. Using digital repeat photography and eddy covariance data to model grassland phenology and photosynthetic $CO_2$ uptake. Agric. For. Meteorol. 151, 1325–1337.
Richardson, A.D., Keenan, T.F., Migliavacca, M., Ryu, Y., Sonnentag, O., Toomey, M., 2013. Climate change, phenology, and phenological control of vegetation feedbacks to the climate system. Agric. For. Meteorol. 169, 156–173.
Running, S.W., Nemani, R.R., Hungerford, R.D., 1987. Extrapolation of synoptic meteorological data in mountainous terrain and its use for simulating forest evapotranspiration and photosynthesis. Can. J. For. Res. 17, 472–483.
Schwartz, M.D., 2013. Phenology: An Integrative Environmental Science. Springer, Dordrecht Heidelberg, New York London.
Shen, M., 2011. Spring phenology was not consistently related to winter warming on the Tibetan Plateau. Proc. Natl. Acad. Sci. U.S.A. 108, E91–E92.
Shen, M., Tang, Y., Chen, J., Zhu, X., Zheng, Y., 2011. Influences of temperature and precipitation before the growing season on spring phenology in grasslands of the central and eastern Qinghai-Tibetan Plateau. Agric. For. Meteorol. 151, 1711–1722.
Shen, M., Piao, S., Dorji, T., Liu, Q., Cong, N., Chen, X., An, S., Wang, S., Wang, T., Zhang, G., 2015b. Plant phenological responses to climate change on the Tibetan Plateau: research status and challenges. Natl. Sci. Rev. 2, 454–467.
Shen, M., Piao, S., Cong, N., Zhang, G., Jassens, I.A., 2015a. Precipitation impacts on vegetation spring phenology on the Tibetan Plateau. Glob. Change Biol. 21, 3647–3656.
Stöckli, R., Rutishauser, T., Dragoni, D., O'Keefe, J., Thornton, P.E., Jolly, M., Lu, L., Denning, A.S., 2008. Remote sensing data assimilation for a prognostic phenology model. J. Geophys. Res. 113, G04021.
Sun, Q., Li, B., Zhang, T., Yuan, Y., Gao, X., Ge, J., Li, F., Zhang, Z., 2017. An improved Biome-BGC model for estimating net primary productivity of alpine meadow on the Qinghai-Tibet Plateau. Ecol. Model. 350, 55–68.
Tetens, O., 1930. About some meteorological terms. Z. Geophys. 6, 297–309.
Thimann, K.V., Satler, S.O., 1979b. Relation between leaf senescence and stomatal opening: senescence in darkness. Proc. Natl. Acad. Sci. U.S.A. 76, 2770–2773.
Thimann, K.V., Satler, S.O., 1979a. Relation between leaf senescence and stomatal closure: senescence in light. Proc. Natl. Acad. Sci. U.S.A. 76, 2295–2298.
Wang, C., Cao, R., Chen, J., Rao, Y., Tang, Y., 2015. Temperature sensitivity of spring vegetation phenology correlates to within-spring warming speed over the Northern Hemisphere. Ecol. Ind. 50, 62–68.
Wang, H., Ma, M., Wang, X., Yuan, W., Song, Y., Tan, J., Huang, G., 2013a. Seasonal variation of vegetation productivity over an alpine meadow in the Qinghai-Tibet Plateau in China: Modeling the interactions of vegetation productivity, phenology, and the soil freeze-thaw process. Ecol. Res. 28, 271–282.
Wang, T., Peng, S., Lin, X., Chang, J., 2013b. Declining snow cover may affect spring phenological trend on the Tibetan Plateau. Proc. Natl. Acad. Sci. U.S.A. 110, E2854–E2855.
Wang, S., Wang, X., Chen, G., Yang, Q., Wang, B., Ma, Y., Shen, M., 2017. Complex responses of spring vegetation phenology to snow cover dynamics over the Tibetan Plateau, China. Sci. Total Environ. 593–594, 449–461.
White, W.A., Thornton, P.E., Running, S.W., 1997. A continental phenology model for monitoring vegetation response to interannual climatic variability. Global Biogeochem. Cycles 11, 217–234.
Yu, H., Luedeling, E., Xu, J., 2010. Winter and spring warming result in delayed spring phenology on the Tibetan Plateau. Proc. Natl. Acad. Sci. U.S.A. 107, 22151–22156.
Zhang, G., Li, X., 1992. Investigation on analysing of the relationship between grass recovery date and ground temperature on South Qinghai Plateau and forecasting methods. Pratac. Sci. 9, 47–51.
Zhang, G., Zhang, Y., Dong, J., Xiao, X., 2013. Green-up dates in the Tibetan Plateau have continuously advanced from 1982 to 2011. Proc. Natl. Acad. Sci. U.S.A. 110, 4309–4314.
Zheng, Z., Zhu, W., Chen, G., Jiang, N., Fan, D., Zhang, D., 2016. Continuous but diverse advancement of spring-summer phenology in response to climate warming across the Qinghai-Tibetan Plateau. Agric. For. Meteorol. 223, 194–202.
Zhou, X.M., 2001. Chinese *Kobresia* Meadow. Science Press, Beijing (in Chinese).
Zhou, H.K., Yao, B.Q., Xu, W.X., Ye, X., Fu, J.J., Jin, Y.X., Zhao, X.Q., 2014. Field evidence for earlier leaf-out dates in alpine grassland on the eastern Tibetan Plateau from 1990 to 2006. Biol. Lett. 10, 1565–1579.
Zhu, W., Jiang, N., Chen, G., Zhang, D., Zheng, Z., Fan, D., 2017. Divergent shifts and responses of plant autumn phenology to climate change on the Qinghai-Tibetan Plateau. Agric. For. Meteorol. 239, 166–175.